

Adsorption configuration effects on the surface diffusion of large organic molecules: The case of Violet Lander

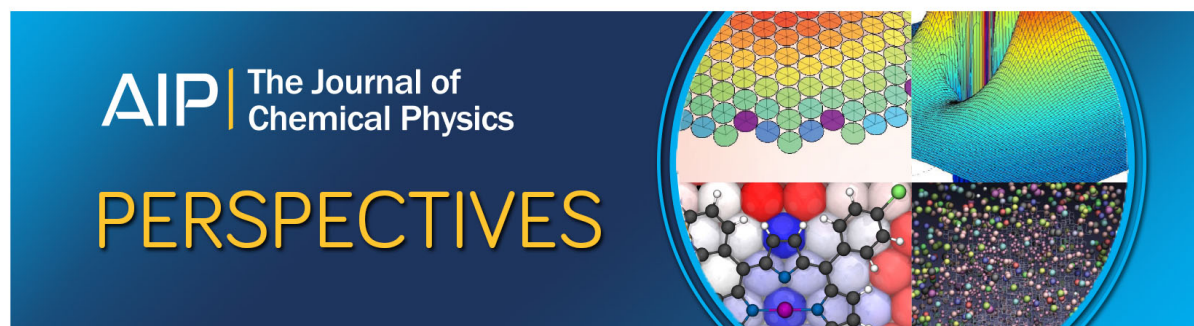
F. Sato, S. B. Legoas, R. Otero, F. Hümmelink, P. Thostrup, E. Lægsgaard, I. Stensgaard, F. Besenbacher, and D. S. Galvão

Citation: *The Journal of Chemical Physics* **133**, 224702 (2010); doi: 10.1063/1.3512623

View online: <https://doi.org/10.1063/1.3512623>

View Table of Contents: <http://aip.scitation.org/toc/jcp/133/22>

Published by the *American Institute of Physics*



Adsorption configuration effects on the surface diffusion of large organic molecules: The case of Violet Lander

F. Sato,¹ S. B. Legoas,² R. Otero,³ F. Hümmelink,⁴ P. Thostrup,⁴ E. Lægsgaard,⁴ I. Stensgaard,⁴ F. Besenbacher,⁴ and D. S. Galvão^{5,a)}

¹Departamento de Física, ICE, Universidade Federal de Juiz de Fora, 36036-330 Juiz de Fora - MG, Brazil

²Departamento de Física, Universidade Federal de Roraima, 69304-000 Boa Vista RR, Brazil

³Departamento de Física, CCT, de la Materia Condensada, Universidad Autónoma de Madrid, Cantoblanco, 28049 Madrid, Spain

⁴Interdisciplinary Nanoscience Center (iNANO) and Department of Physics and Astronomy, University of Aarhus, DK-8000 Aarhus C, Denmark

⁵Instituto de Física “Gleb Wataghin,” Universidade Estadual de Campinas, C. P. 6165, 13083-970 Campinas SP, Brazil

(Received 21 July 2010; accepted 15 October 2010; published online 10 December 2010)

Violet Lander ($C_{108}H_{104}$) is a large organic molecule that when deposited on Cu(110) surface exhibits lock-and-key like behavior [Otero *et al.*, *Nature Mater.* **3**, 779 (2004)]. In this work, we report a detailed fully atomistic molecular mechanics and molecular dynamics study of this phenomenon. Our results show that it has its physical basis on the interplay of the molecular hydrogens and the Cu(110) atomic spacing, which is a direct consequence of the matching between molecule and surface dimensions. This information could be used to find new molecules capable of displaying lock-and-key behavior with new potential applications in nanotechnology. © 2010 American Institute of Physics. [doi:10.1063/1.3512623]

I. INTRODUCTION

With the advent of nanoscience and nanotechnology and the perspective of molecular electronics,^{1–7} significant theoretical and experimental efforts have been devoted to the study of the complex interactions involving organic molecular structures and metallic surfaces.^{8–26} One essential aspect of these phenomena is to understand how these interactions alter the properties of both molecule and surface. Recent progress has been achieved through the use of ultrahigh vacuum-scanning tunneling microscopy^{11,27} that allowed the identification of important structural and dynamical features related to the behavior of molecular wires adsorbed on metallic surfaces.

One important family of molecular wires is the so-called “Lander molecules” (because of its resemblance to the Mars surface rover).^{28–33} These large organic molecules are composed of a rigid polyaromatic π central board and four spacers (*legs*) of up to eight 3,5-di-*tert*-butylphenyl groups, σ -bonded to the central board (Fig. 1). These spacers generate a configuration where the phenyl groups are nearly perpendicular to the main board plane by steric crowding. Also, the board-surface distance is increased by these *tert*-butyl groups. When deposited onto a metallic surface, the board is decoupled from the surface by the spacer legs, making it not visible in STM experiments. However, there is an electronic interaction between the π orbitals of the Lander board and surface states, which converts the board in a scattering center for surface state electrons.³⁴

When adsorbed on Cu(100) or Cu(110) surfaces, the Lander molecule can act as a template for self-accommodating metal atoms at the step edges of the copper substrate, spontaneously generating metallic nanostructures dimensionally compatible with the Landers.^{16,35} This phenomenon opens up interesting possibilities for the bottom-up design of metallic nanostructures.

Similar studies for other molecules of the Lander family, the so-called Violet Lander (VL) (violet due to its color)— $C_{108}H_{104}$ —led to the observation in the solid state of the first nonbiological lock-and-key like effect.³⁶ A change by 2 orders of magnitude of the diffusion coefficients was observed when the molecular orientation of the substrate was changed. Previous experimental and theoretical investigations^{16,36,37} have revealed that VL molecules adsorb at room temperature (RT) on the Cu(110) surface with the polyaromatic board parallel to the substrate and aligned along the $[1\bar{1}0]$ direction (parallel configuration) [Figs. 2(a) and 2(c)]. In this configuration, the molecules do not diffuse during the STM observation time (several minutes). The estimated diffusion coefficient is less than $5 \times 10^{-19} \text{ cm}^2 \text{ s}^{-1}$.³⁶

When the STM tip is used as a tool to push the adsorbed molecule onto the copper surface at low temperatures (160–200 K),³⁶ the molecule rotates 70° (from the $[1\bar{1}0]$ direction) [Figs. 2(b) and 2(d)], and then it diffuses along the $[1\bar{1}0]$ direction with an estimated diffusion coefficient of $4.8 \times 10^{-17} \text{ cm}^2 \text{ s}^{-1}$.³⁶ This represents an increase of 2 orders of magnitude with relation to the parallel configuration. Interestingly, this molecular diffusion can be stopped at any time simply by flipping the molecule back to its parallel configuration. These two distinct configurations work as a two-state system (0 and 1 / *on* and *off*), and it is the phenomenon analogous

^{a)} Author to whom correspondence should be addressed. Electronic mail: galvao@ifi.unicamp.br.

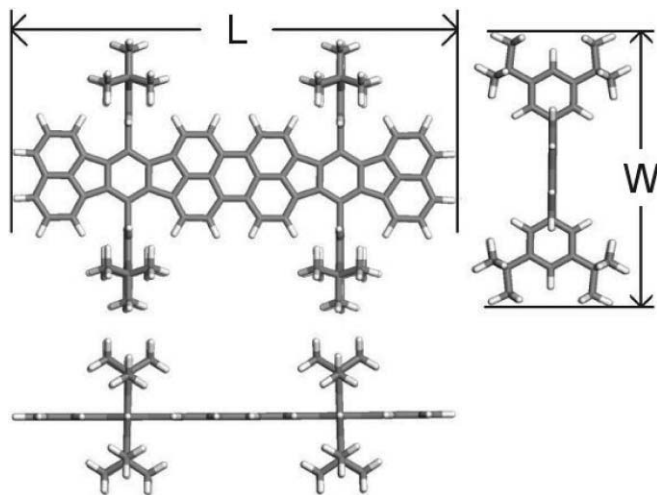


FIG. 1. Structural representation of the Violet Lander ($C_{108}H_{104}$) along different direction views. The experimental and theoretical values of the major molecular dimensions L and W are displayed in Table 1 (see text for discussions).

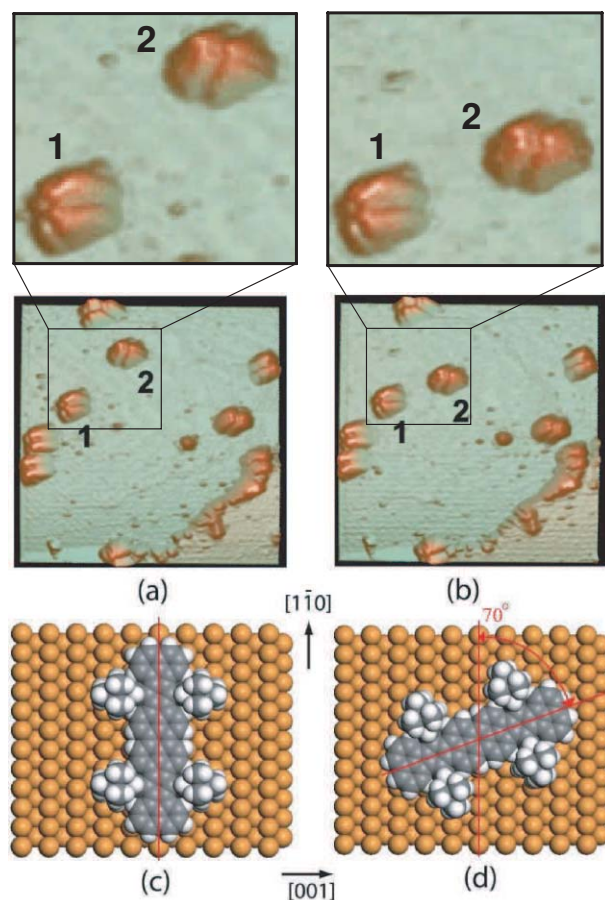


FIG. 2. STM snapshots from the scanning of VL molecules adsorbed on Cu(110) surface. (a) and (b) Molecules with their main boards aligned with the $[1\bar{1}0]$ direction (labeled 1) do not diffuse; molecules rotated by 70° (labeled 2) are able to diffuse along the $[1\bar{1}0]$ direction. In the upper panels are showed zoomed images of rectangular sections of (a) and (b), respectively. (c) and (d) 3D-graphical atomistic representation of the VL in its (c) aligned and (d) 70° rotated configurations with respect to the $[1\bar{1}0]$ Cu(110) surface direction. The STM images represent raw data, no image processing was done after acquisition.

of the so-called *biological lock-and-key* recognition between enzymes and the substrate on which they act.³⁸

Surprisingly, in spite of many years of investigations into the diffusion of organic molecules on metallic surfaces, this phenomenon had not been observed before. As we shall see in the following discussions, its physical roots are based on the matching of the VL with the atomic spacing of the Cu(110). Changing the molecule and/or the crystallographic direction, the phenomenon will not be observed. In this work, we present a detailed fully atomistic molecular mechanics and molecular dynamics study of the diffusion process of VL molecules adsorbed on a Cu(110) surface.

II. METHODOLOGY

We carried out molecular mechanics and impulse molecular dynamics calculations in the framework of classical mechanics with standard force field [universal force field (UFF)],³⁹ which includes van der Waals, bond stretch, bond angle bend, and torsional rotation terms. This methodology has been proven to be very effective for the study of structural and dynamical properties of complex structures.^{40–43}

For all simulations, the following convergence criteria were used:^{44,45} maximum force of 0.005 kcal/mol/Å, root-mean-square (RMS) deviations of 0.001 kcal/mol/Å, energy differences of 0.0001 kcal/mol, maximum atomic displacement of 0.000 05 Å, and RMS displacement of 0.000 01 Å. A selective microcanonical (constant number of particles, volume, and total energy) impulse dynamics was used, with time steps of 1 fs.

Initially, the VL molecule was optimized in the gas phase (isolated). The use of full quantum methods for the whole system is not possible due to its large size, but the calculation for the isolated molecules is possible. In order to test the UFF quality for the geometrical results of the molecular structures, we have carried out a series of calculations using different methods, for comparison purposes: the semiempirical Hamiltonian AM1 available in the GAMESS package,⁴⁶ and the *ab initio* density functional methods Siesta^{47,48} and state-of-the-art DMol³,^{49–51} using the local density approximation (LDA).

The DMol³ calculations were carried out considering the Wang–Perdew exchange-correlation functional (PWC),⁵² and the core electrons were treated in a nonrelativistic all-electron implementation of the potential. A double numerical quality basis set, with polarization functions, was considered with a cutoff radius of 3.7 Å. For the Siesta calculations, we have used the standard double zeta plus polarization basis, with an energy shift of 0.27 eV. A cutoff of 180.0 Ry for the grid integration was used in order to represent the electronic charge density using the local LDA-CA/PZ functional.⁵³ The pseudopotential was constructed following the Troullier–Martins scheme.⁵⁴

The obtained structural dimensions are very consistent and in very good agreement with the estimated experimental data from STM experiments,^{16,36,55–57} indicating that the used molecular force field reproduces the VL geometrical features quite well (see Table I).

TABLE I. Violet Lander dimensions (Fig. 1), in angstrom, optimized with classical molecular mechanics [universal force field (Ref. 39)], semiempirical AM1 method (Ref. 46), DFT-LDA-Siesta (Refs. 47 and 48), and DFT-LDA-DMol³ (Refs. 49–51).

| Method | L | W |
|---------------------|-------|-------|
| Molecular mechanics | 25.34 | 15.45 |
| AM1 | 25.35 | 15.45 |
| Siesta | 25.25 | 15.48 |
| DMol3 | 25.16 | 15.36 |

We then proceed with UFF calculations. The molecule with its board parallel to the Cu(110) surface is placed (about $\sim 4\text{--}6$ Å) above the surface and set free to interact with the surface. We have also considered the cases where a small vertical impulse was given to the molecules to move them toward the surface. This is an additional test in order to provide enough kinetic energy to probe local minima. These procedures were repeated varying the relative angular orientation and the geometries reoptimized. As the copper surfaces do not reconstruct, the Cu atoms were kept frozen at the experimental lattice value of $a = 3.61$ Å.⁵⁸ For the impulse molecular dynamics, the molecules are placed in one of the most stable configurations (rotated/nonrotated) and given an initial velocity along specific directions and we then analyze their time evolution (force and energy profiles). In all our simulations, the “legs” were set completely free to rotate and/or distort.

III. RESULTS AND DISCUSSIONS

Our results showed that the molecules always converge to two possible configurations, 0° and 70° with respect to the $[1\bar{1}0]$ orientation. In order to better understand this problem, we mapped the energy configuration as a function of the rotation angles. For comparative purposes, this was carried out in two different ways: the molecule was placed at 0° , initially with its board frozen (in order to keep it at the specified angle value) but with all remaining geometrical variables free to vary. Then its geometry is optimized. The molecule is then rotated in steps of 5° and the process is repeated to obtain the rotational energy profile. This procedure was also carried out keeping frozen just the central ring of the molecular board, in order to verify if this would significantly affect the energy profiles. The results for the two different procedures are displayed in Fig. 3, and they are very similar. We observed that in fact the two most stable configurations are at 0° and 70° (in agreement with the experimental data),³⁶ with a difference in energy of 0.75 kcal/mol. A third minimum was obtained for about 30° . This third stable configuration was not experimentally observed. This can be explained by the fact that the temperatures considered in the experiments can provide sufficient thermal energy to overcome this small depth/width energy local minima.

We repeated the process (frozen central ring and steps of 5°) on Cu(100) and Cu(111) surfaces. The results are displayed in Fig. 4. As we can see from Fig. 4, in contrast to the (110) surface (Fig. 3), the energy peaks and valleys are

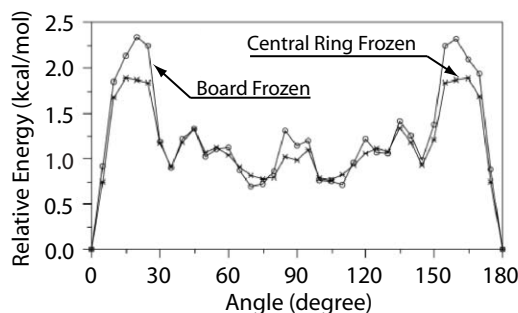


FIG. 3. Relative total energy profile of a VL molecule deposited on a Cu(110) surface as a function of the angle between the main axis of the molecule and the $[1\bar{1}0]$ direction (see Fig. 2). For each angle, the molecule is optimized with its board or central ring being frozen.

smaller and smoother. No well defined constrained configuration was obtained. We observed in the simulations that these valleys and peaks could be easily thermally overcome, which prevents the lock-key like phenomenon observed for the (110) surface to occur.

The results show that the energy necessary for the diffusion on Cu(110) surface, in the nonrotated case, is much higher (~ 0.7 kcal/mol) than in the rotated case (~ 0.05 kcal/mol), and beyond the thermally available energy of the temperature at which the experiments are realized. For the rotated case, the energy necessary is thermally available.

Similarly to the rotational analysis (Fig. 3), we have also mapped the translational movement (keeping only the central board ring frozen) for the rotated and nonrotated configurations on the Cu(110) surface. Due to energy profile mentioned above, the translational mappings do not provide new relevant information about the (100) and (111) surfaces.

The molecules were moved in steps of 0.1 Å along the $[1\bar{1}0]$ direction, and for each point the geometry is optimized. The results are displayed in Fig. 5. We observed that the energies associated with the movements of nonrotated and rotated cases are quite different, being higher for the nonrotated case. From Fig. 5, it is possible to explain why the molecules can easily diffuse in the rotated case. The reason for this being that we have a very low energy barrier for diffusion. However, although the barrier is much higher in the nonrotated case than in the rotated case, its absolute value is not high enough to prevent the overcoming of the potential energy barrier by kinetic energy. Static analyses have been often used in

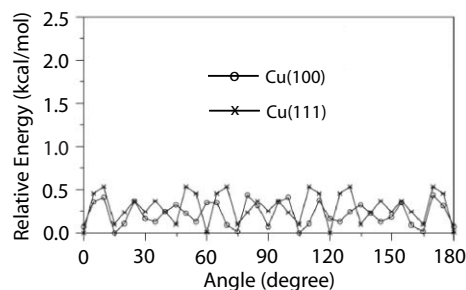


FIG. 4. Relative total energy profile of a VL molecule deposited on Cu(100) and Cu(111) surfaces as a function of the angle between the molecule main axis and the $[010]$ and $[1\bar{1}1]$ directions, respectively.

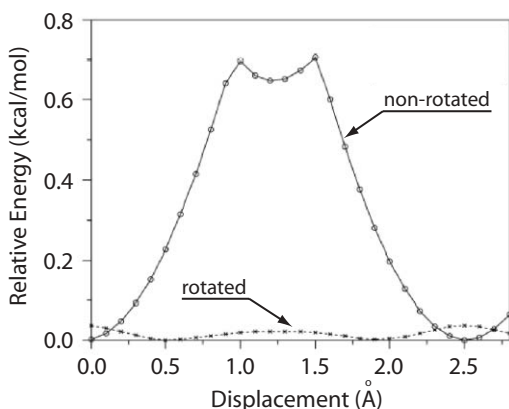


FIG. 5. Energy profile for the VL molecule displacement onto the Cu(110) surface, along the $[1\bar{1}0]$ direction in the rotated and nonrotated geometries.

the literature to explain diffusion problems. In the present case although they provided helpful information, the obtained data seem to be insufficient to explain whole set of experimental data of the dynamics diffusion and suggest that the dynamical aspects must be explicitly taken into account. These aspects have not been properly addressed before in the literature and might be of importance for the surface science of large organic adsorbates.^{35,36}

A deeper understanding of the molecular diffusion can be obtained from the analysis of the temporal evolution through impulse molecular dynamics simulations where the information about the force profile and molecular conformational changes can be easily addressed in femto second scale (which is not possible in the experimental case).

We simulated the VL diffusion over Cu(110) surface using impulse molecular dynamics protocols. We attributed an initial velocity (impulse) to the molecules and followed the time evolution of their dynamics variable (positions, velocities, forces). From these variables, it is possible to estimate the relative diffusion coefficients.⁵⁹ The procedure of using an initial impulse is to mimic thermal effects and/or tip “kick” applied to the molecules. Another reason is to allow the simulations to be carried out in a feasible computer time. We have considered the cases of the nonrotated and rotated configurations. In each case, different impulse velocities were used to determine the threshold values to induce molecular movements along the $[1\bar{1}0]$ direction. For the nonrotated case, we concluded that initial values larger than 0.9 Å/ps (equivalent to a kinetic energy of 1.36 kcal/mol) are necessary to induce molecular diffusion. On the other hand, for the rotated case only values of 0.4 Å/ps (equivalent to 0.27 kcal/mol) are required.

In Fig. 6, we present the force profiles as a function of time of the forces experienced by the molecule for the different configurations. The displayed data are for a situation where the initial impulse velocities were set up to 0.8 Å/ps along the $[1\bar{1}0]$ direction (see complementary material video 01).⁶⁰ For the nonrotated configuration [Fig. 6(a)], in the first $\sim 1.8 \text{ ps}$ the force exerted on the molecule attains high values, near to 20 pN along the opposite direction of the applied initial impulse. The force values decrease very fast ($\sim 5.0 \text{ pN}$ at 5.0 ps and $< 2.5 \text{ pN}$ at 15 ps), as the initial

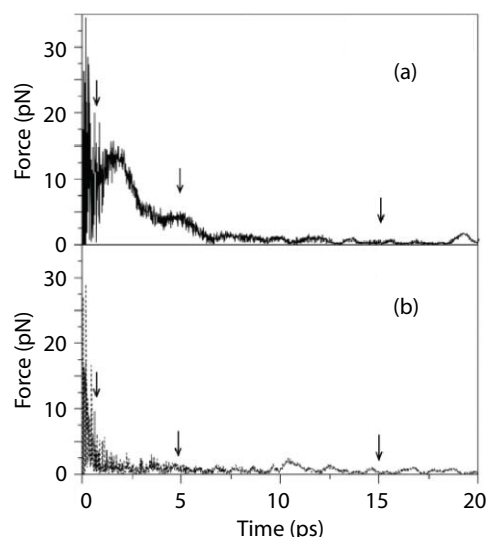


FIG. 6. Force profile, as a function of time, as a result of the interaction between the VL molecule in the (a) nonrotated and (b) rotated geometries, and the Cu(110) surface. Times corresponding to 1.8, 4.8, and 15 ps as a result of the initial impulse are shown by arrows.

translational energy is converted into vibrational and torsional molecular movements. The molecule oscillates back and forth around its initial position, but no diffusion (net displacement) is observed (see video 01). The situation is quite different for the rotated case [Fig. 6(b)]. The initial forces are quickly attenuated, and the molecule easily diffuses (see video 01).

From the video 01, we can clearly see that for the nonrotated case the molecule oscillates back and forth without diffusing. This oscillatory behavior can also be seen in the root mean displacement (RMD) data (Fig. 7). The associated RMD diffusion coefficients⁶¹ are $9.1 \times 10^{-6} \text{ cm}^2 \text{ s}^{-1}$ and $5.6 \times 10^{-4} \text{ cm}^2 \text{ s}^{-1}$ for the nonrotated and rotated cases, respectively. These diffusion coefficients are obtained from the analysis of the impulse molecular dynamics trajectory simulations where the initial impulse kinetic energy is quickly redistributed to the torsion/vibration/deformation-lengths molecular modes. In the experiments after the initial “tip kick,” the nonrotated molecule undergoes an orientational transition to the rotated configuration, and due to the available thermal bath it has enough kinetic energy to diffuse. Although the absolute values of the theoretical and experimental diffusion

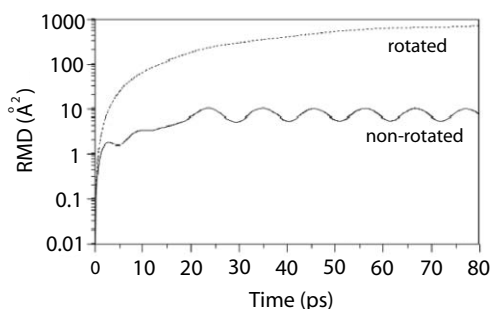


FIG. 7. Root mean displacement (RMD) of rotated (dot pointed curve) and nonrotated (fill curve) VL. The diffusion coefficient associated from curves are $9.1 \times 10^{-6} \text{ cm}^2/\text{s}$ and $5.6 \times 10^{-4} \text{ cm}^2/\text{s}$ for nonrotated and rotated VL, respectively.

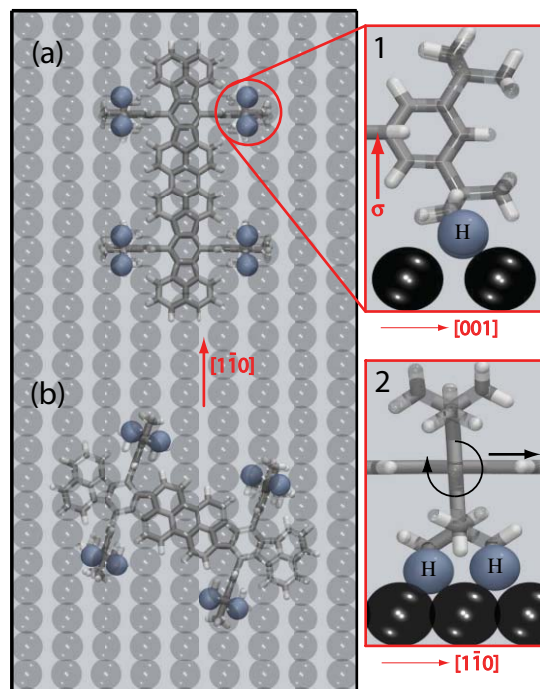


FIG. 8. Schematic view of a VL molecule in its (a) nonrotated and (b) 70° rotated configurations with respect to the $[1\bar{1}0]$ Cu(110) surface direction. Insets 1 and 2 show structural details of the hydrogen atoms fitting into the hollow sites of the Cu(110) surface, in the nonrotated geometry. When the board slides, the legs rotate easily around the sigma bonds (σ) inducing the hydrogen atoms (H) to remain in the hollow sites.

coefficients cannot be directly compared, their relative differences can. They are in excellent agreement showing the same 2 orders of magnitude differences, $9.1 \times 10^{-6} \text{ cm}^2 \text{ s}^{-1}$ and $5.6 \times 10^{-4} \text{ cm}^2 \text{ s}^{-1}$ versus $5.0 \times 10^{-19} \text{ cm}^2 \text{ s}^{-1}$ and $4.8 \times 10^{-17} \text{ cm}^2 \text{ s}^{-1}$ for the nonrotated and rotated case, theoretical and experimental values, respectively, i.e., a difference by a factor of 100.

From the molecular conformational changes as a function of time, it is possible to obtain helpful information about the dynamics of the diffusion processes. The relative position of the hydrogen atoms of the molecular legs in relation to the copper (110) direction plays a fundamental role in defining whether diffusion is possible or not.

The VL adsorbed on the Cu(110) substrate exposes eight hydrogen atoms at the bottom of the legs. In the nonrotated configuration, these H atoms fit perfectly (“locked”) into the fourfold hollow sites of Cu(110) [Fig. 8(a)]. Due to this perfect fitting, despite the freedom of the legs to rotate around the sigma-bonds of the board, any tentative translational given energy is more likely to be converted into conformational changes than into net displacement (video 01), thus blocking diffusion. For the rotated configuration, as the fitting is not as good [Figs. 8(a) and 8(b)], translational energy is easily converted into kinetic energy, and diffusion is possible.

It is important to stress that the configuration for which the diffusion is blocked, is just a consequence of the compatibility between the distance of the legs and the atomic spacing of Cu(110). For instance, for the Cu(100) and Cu(111) substrates the spacing is no longer compatible with the legs distances and the perfect “fitting” does not occur. Conse-

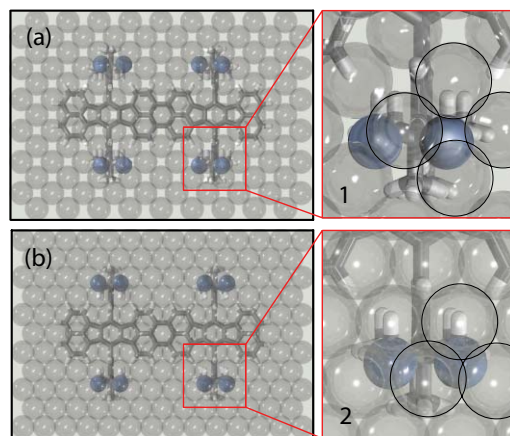


FIG. 9. Schematic view of the VL molecule for the nonrotated configuration on (a) Cu(100) and (b) Cu(111) surfaces, respectively. The different hydrogen atom orientations in relation to the Cu surface atoms are clearly visible. Insets 1 and 2 show detailed views of the poor matching between the hydrogen atoms at the bottom of the legs and the hollow sites of Cu(100) and Cu(111) surfaces, respectively. In comparison with the Cu(110) (Fig. 8), the hollow sites of Cu(100) and Cu(111) are shallower.

quently, the lock-and-key like effect will not be observed (Fig. 9). The existence of the “fortuitous” matching in the case of VL/Cu(110) might explain why this lock-key like effect was not observed before, in spite of many years of investigations of the diffusion patterns of large organic molecules over metallic substrates.¹⁸

IV. SUMMARY AND CONCLUSIONS

We report here a detailed fully atomistic molecular mechanics and impulse molecular dynamics study of the diffusion process of VL molecules adsorbed on different Cu substrates [(111), (100), and (110)], in the framework of classical mechanics with standard force field UFF.³⁹ Quantum method calculations (semiempirical and *ab initio* density functional theory) for the isolated molecules were also carried out in order to test the quality of geometries obtained with UFF. The results showed an excellent agreement between the different methods and the experimental data (see Table I).

For the molecules deposited on the Cu substrates, we carried out both, static and dynamical calculations, of the VL-molecule/substrate interactions in order to identify the origin of the lock-and-key like effect observed for Cu(110). Both energy and force profiles reveal that the diffusion coefficient difference of VL molecule on Cu(110) surface is due to a compatibility/incompatibility geometrical aspect of the organic molecule with respect to the $[1\bar{1}0]$ direction of the substrate.

In this sense, it is possible to consider the existence of other structures (satisfying the criteria of no significant charge transfer between the molecule and the substrate and “matching” the geometrical conditions) that could exhibit the same adsorption configuration phenomenon observed for Violet Lander.

As VL molecules proved to be capable of exhibiting many interesting properties (such as spontaneously building ordered nanostructures), these results can be of great

relevance to build nanostructures in a bottom-up approach. We hope the present study will stimulate further studies along these lines.

ACKNOWLEDGMENTS

This work was supported in part by the Brazilian Agencies CNPq, CAPES, FAPEMIG, and FAPESP.

- ¹J. K. Gimzewski and C. Joachim, *Science* **283**, 1683 (1999).
- ²C. Joachim, J. K. Gimzewski, and A. Aviram, *Nature* **408**, 541 (2000).
- ³C. Cai, M. M. Bösch, B. Müller, Y. Tao, A. Kündig, C. Bosshard, Z. Gan, I. Biaggio, I. Liakatas, M. Jäger, H. Schwer, and P. Günter, *Adv. Mater.* **11**, 745 (1999).
- ⁴A. Kühnle, T. R. Linderoth, B. Hammer, and F. Besenbacher, *Nature* **415**, 891 (2002).
- ⁵E. E. Oren, C. Tamerler, and M. Sarikaya, *Nano Lett.* **5**, 415 (2005).
- ⁶H. P. Lang, M. Hegner, E. Meyer, and C. Gerber, *Nanotechnology* **13**, R29 (2002).
- ⁷F. Moresco, G. Meyer, and K.-H. Rieder, *Phys. Rev. Lett.* **86**, 672 (2001).
- ⁸T. Yokoyama, S. Yokoyama, T. Kamikado, Y. Okuno, and S. Mashiko, *Nature* **413**, 619 (2001).
- ⁹T. Zambelli, P. Jiang, J. Lagoute, S. E. Grillo, S. Gauthier, A. Gourdon, and C. Joachim, *Phys. Rev. B* **66**, 075410 (2002).
- ¹⁰F. Rosei, M. Schunack, Y. Naitoh, P. Jiang, A. Gourdon, E. Lægsgaard, I. Stensgaard, C. Joachim, and F. Besenbacher, *Prog. Surf. Sci.* **71**, 95 (2003).
- ¹¹F. Rosei, M. Schunack, P. Jiang, A. Gourdon, E. Lægsgaard, I. Stensgaard, C. Joachim, and F. Besenbacher, *Science* **296**, 328 (2002).
- ¹²F. Moresco, L. Gross, M. Alemani, K.-H. Rieder, H. Tang, A. Gourdon, and C. Joachim, *Phys. Rev. Lett.* **91**, 036601 (2003).
- ¹³J. V. Barth, *Angew. Chem., Int. Ed. Engl.* **39**, 1230 (2000).
- ¹⁴J. A. Theobald, N. S. Oxtoby, M. A. Phillips, N. R. Champness, and P. H. Beton, *Nature* **424**, 1029 (2003).
- ¹⁵M. Eremitchenko, J. A. Schaefer, and F. S. Tautz, *Nature* **425**, 602 (2003).
- ¹⁶R. Otero, F. Rosei, Y. Naitoh, P. Jiang, P. Thstrup, A. Gourdon, E. Lægsgaard, I. Stensgaard, C. Joachim, and F. Besenbacher, *Nano Lett.* **4**, 75 (2004).
- ¹⁷J. Kuntze, X. Ge, and R. Berndt, *Nanotechnology* **15**, S337 (2004).
- ¹⁸F. Moresco, *Phys. Rep.* **399**, 175 (2004).
- ¹⁹K.-Y. Kwon, K. L. Wong, G. Pawin, L. Bartels, S. Stolrov, and T. S. Rahman, *Phys. Rev. Lett.* **95**, 166101 (2005).
- ²⁰L. Grill, K.-H. Rieder, F. Moresco, S. Stojkovic, A. Gourdon, and C. Joachim, *Nano Lett.* **6**, 2685 (2006).
- ²¹S. Weigelt, C. Busse, L. Petersen, E. Rauls, B. Hammer, K. V. Gothelf, F. Besenbacher, and T. R. Linderoth, *Nature Mater.* **5**, 112 (2006).
- ²²X. Ge, J. Kuntze, R. Berndt, H. Tang, and A. Gourdon, *Chem. Phys. Lett.* **458**, 161 (2008).
- ²³M. Yu, W. Xu, Y. Benjalal, R. Barattin, E. Lægsgaard, I. Stensgaard, M. Hliwa, X. Bouju, A. Gourdon, C. Joachim, T. R. Linderoth, and F. Besenbacher, *Nano. Res.* **2**, 254 (2009).
- ²⁴S. Kuck, S.-H. Chang, J.-P. Klöckner, M. H. Prosenc, G. Hoffmann, and R. Wiesendanger, *ChemPhysChem* **10**, 2008 (2009).
- ²⁵S. Godlewski, G. Goryl, A. Gourdon, J. J. Kolodziej, B. Such, and M. Szymonski, *ChemPhysChem* **10**, 2026 (2009).
- ²⁶L. Grill, *J. Phys.: Condens. Matter* **22**, 084023 (2010).
- ²⁷M. Schunack, F. Rosei, Y. Naitoh, P. Jiang, A. Gourdon, E. Lægsgaard, I. Stensgaard, C. Joachim, and F. Besenbacher, *J. Chem. Phys.* **117**, 6259 (2002).
- ²⁸S. C. Ghosh, X. Zhu, A. Secchi, S. K. Sadhukhan, N. K. Girdhar, and A. Gourdon, *Ann. N.Y. Acad. Sci.* **1006**, 82 (2003).
- ²⁹A. Gourdon, *Eur. J. Org. Chem.* 2797 (1998).
- ³⁰V. J. Langlais, R. R. Schlittler, H. Tang, A. Gourdon, C. Joachim, and J. K. Gimzewski, *Phys. Rev. Lett.* **83**, 2809 (1999).
- ³¹J. Kuntze, R. Berndt, P. Jiang, H. Tang, A. Gourdon, and C. Joachim, *Phys. Rev. B* **65**, 233405 (2002).
- ³²L. Gross, F. Moresco, M. Alemani, H. Tang, A. Gourdon, C. Joachim, and K.-H. Rieder, *Chem. Phys. Lett.* **371**, 750 (2003).
- ³³L. Grill, K.-H. Rieder, F. Moresco, S. Stojkovic, A. Gourdon, and C. Joachim, *Nano Lett.* **5**, 859 (2005).
- ³⁴L. Gross, F. Moresco, L. Savio, A. Gourdon, C. Joachim, and K.-H. Rieder, *Phys. Rev. Lett.* **93**, 056103 (2004).
- ³⁵R. Otero, F. Rosei, and F. Besenbacher, *Annu. Rev. Phys. Chem.* **57**, 497 (2006).
- ³⁶R. Otero, F. Hümmlink, F. Sato, S. B. Legoas, P. Thstrup, E. Lægsgaard, I. Stensgaard, D. S. Galvão, and F. Besenbacher, *Nature Mater.* **3**, 779 (2004).
- ³⁷T. Zambelli, H. Tang, J. Lagoute, S. Gauthier, A. Gourdon, and C. Joachim, *Chem. Phys. Lett.* **348**, 1 (2001).
- ³⁸L. Stryer, *Biochemistry* (W. H. Freeman, New York, 1997).
- ³⁹UNIVERSAL1.02 molecular force field, available from Accelrys, Inc. as part of Materials Studio and Cerius2 program suites. <http://www.accelrys.com>.
- ⁴⁰S. B. Legoas, V. R. Coluci, S. F. Braga, P. Z. Coura, S. O. Dantas, and D. S. Galvão, *Phys. Rev. Lett.* **90**, 055504 (2003); *Nanotechnology* **15**, S184 (2004).
- ⁴¹S. B. Legoas, R. Giro, and D. S. Galvão, *Chem. Phys. Lett.* **386**, 425 (2004).
- ⁴²S. F. Braga, V. R. Coluci, S. B. Legoas, R. Giro, D. S. Galvão, and R. H. Baughman, *Nano Lett.* **4**, 881 (2004).
- ⁴³R. H. Baughman and D. S. Galvão, *Nature (London)* **365**, 735 (1993).
- ⁴⁴R. Giro and M. J. Caldas, *Phys. Rev. B* **76**, 161303 (2007).
- ⁴⁵R. Giro and M. J. Caldas, *Phys. Rev. B* **78**, 155312 (2008).
- ⁴⁶M. W. Schmidt, K. K. Baldrige, J. A. Boatz, S. T. Elbert, M. S. Gordon, J. H. Jensen, S. Koseki, N. Matsunaga, K. A. Nguyen, S. J. Su, T. L. Windus, M. Dupuis, and J. A. Montgomery, *J. Comput. Chem.* **14**, 1347 (1993), <http://www.msg.ameslab.gov/GAMESS/GAMESS.html>.
- ⁴⁷P. Ordejón, E. Artacho, and M. Soler, *Phys. Rev. B* **53**, 10441 (1996), Siesta Program; version 1.3f1p; <http://www.uam.es/siesta>.
- ⁴⁸D. Sánchez-Portal, P. Ordejón, and E. Canadell, *Structure and Bonding*, **113**, 103 (2004).
- ⁴⁹B. Delley, *J. Chem. Phys.* **92**, 508 (1990).
- ⁵⁰B. Delley, *J. Chem. Phys.* **113**, (7756), (2000).
- ⁵¹DMol3, available from Accelrys, Inc. as part of Materials Studio and Cerius2 program suites. <http://www.accelrys.com>.
- ⁵²J. P. Perdew and Y. Wang, *Phys. Rev. B* **45**, 13244 (1992).
- ⁵³J. P. Perdew and A. Zunger, *Phys. Rev. B* **23**, 5048 (1981).
- ⁵⁴N. Troullier and J. L. Martins, *Phys. Rev. B* **43**, 1993 (1991).
- ⁵⁵L. Savio, F. Moresco, L. Gross, A. Gourdon, C. Joachim, and K.-H. Rieder, *Surf. Sci.* **585**, 38 (2005).
- ⁵⁶L. Savio, L. Gross, K. Rieder, A. Gourdon, C. Joachim, F. Moresco, *Chem. Phys. Lett.* **428**, 331 (2006).
- ⁵⁷R. Otero, Y. Naitoh, F. Rosei, P. Jiang, P. Thstrup, A. Gourdon, E. Lægsgaard, I. Stensgaard, C. Joachim, and F. Besenbacher, *Ang. Chem. Int. Ed.* **43**, 2092 (2004).
- ⁵⁸W. B. Pearson, *A Handbook of Lattice Spacings and Structures of Metals and Alloys* (Pergamon, New York, 1964), Vol. 1.
- ⁵⁹M. E. Tuckerman, *Statistical Mechanics: Theory and Molecular Simulation* (Oxford University, New York, 2010), Chap. 13.
- ⁶⁰See supplementary material at <http://dx.doi.org/10.1063/1.3512623> for the movie mentioned in the text.
- ⁶¹The diffusion coefficients were obtained from the root mean displacement data with a least squares straight line fitting using the Einstein relation, see R. Chitra and S. Yashonath, *J. Phys. Chem. B* **101**, 5437 (1997).